

GENERALIZED LIKELIHOOD RATIO TEST FOR FINITE MIXTURE MODEL OF K-DISTRIBUTED RANDOM VARIABLES

*J. Derek Tucker, J. Tory Cobb**

Naval Surface Warfare Center
Panama City Division
Panama City, Florida 32407-7001
{james.d.tucker,james.cobb}@navy.mil

Mahmood R. Azimi-Sadjadi

Colorado State University
Department of Electrical and Computer Engineering
Fort Collins, Colorado 80523-1373
azimi@engr.colostate.edu

ABSTRACT

In this paper a new detection method for sonar imagery is developed for \mathcal{K} -distributed background clutter using a finite mixture model (FMM) of \mathcal{K} -distributions. The method for estimation of the parameters of the FMM and a generalized log-likelihood ratio test is derived. The detector is compared to the corresponding counterparts derived for the standard \mathcal{K} -, Gaussian, and Rayleigh distributions. Test results of the proposed method on a data set of synthetic aperture sonar (SAS) images is also presented. This database contains images with synthetically generated targets of different shapes inserted into real SAS background imagery. Results illustrating the effectiveness of the FMM \mathcal{K} -distributed detector are presented in terms of probability of detection, false alarm rates, and receiver operating characteristic (ROC) curves for various bottom clutter conditions.

Index Terms— Binary hypothesis testing, \mathcal{K} -distributed clutter, non-Gaussian signal detection, sonar imagery, underwater target detection

1. INTRODUCTION

The problem of underwater object detection in sonar imagery has recently attracted a substantial amount of attention [1–6]. This problem is complicated due to various factors such as variations in operating and environmental conditions, presence of spatially varying clutter, and variations in target shapes, compositions, and orientations. Moreover, bottom features such as coral reefs, sand formations, and vegetation may totally obscure a target or confuse the detection process. Consequently, a robust detection system should be able to quantify changes between the returns from the sea bottom and targets and mitigate false alarms in various clutter density scenarios.

Considerable research has been devoted to the development of different detection and classification methodologies for underwater sonar imagery. Dobeck [2, 3] utilized a nonlinear matched filter to detect target-size regions that match the target template in a side-scan sonar image. For each detected region, several features were extracted based on the size, shape, and strength of the target template. A stepwise feature selection process was then used to determine the subset of features that maximizes the probability of detection and classification. A k -nearest neighbor and an optimal discrimination filter classifier were used to classify each feature vector and the decisions of the two classifiers were fused to generate the final

decision. In [7], a method was proposed that first median filters the sonar image to reduce the speckle noise. The image was then split into overlapping range segments where the pixels in each segment were adaptively thresholded. The threshold was determined from cumulative distribution function (CDF) formed from a training set. Geometric features were then extracted from contiguous target structure regions within the segment followed by classification of each region as target or non-target using a multi-level weighted scoring-based classification system. In [8], the adaptive clutter filter detector in [9] was individually applied to three different sonar images varying in frequency and bandwidth. Final classification is done using an optimal set of features using the log-likelihood ratio test where the decisions of the individual detector and classifier are fused. Vera recently presented [10] a detection and classification method based on the Hilbert transform, where he used the transformed image to detect highlight and shadow combinations. Geometrical features were then extracted and subsequently classified using a classification tree. Recently in [6] we developed a formulation of the log-likelihood ratio for the \mathcal{K} -distribution which produced good detection results on synthetically generated sonar imagery.

Most statistical-based detection methods rely on the Gaussian assumption of both signal and background noise. Due to this assumption, one is not able to accurately represent sonar bottom clutter and hence the performance gain is sacrificed in the detection process. This is due to the fact that recent studies on bottom clutter statistics reveal [11–13] that the distribution of the envelope of the matched filtered output is dependent on the frequency, grazing angle, range and roughness properties of the bottom. Rough surface measurements made using a high resolution sonar have indicated that the envelope amplitude distributions can be modeled by Rayleigh, log-normal, Weibull or other more complex distributions such as the \mathcal{K} -distribution [12]. This suggests that the underlying complex data is not Gaussian and that second-order moments will not be sufficient for detection purposes, thus impairing the overall performance. This motivates our interest in using a non-Gaussian background model. In [13], the authors used a texture model based on the correlated \mathcal{K} -distribution to model seabed textures in sonar imagery. Model parameters are estimated from a set of textured sonar images using a method based on Expectation Maximization (EM) for truncated data [14]. The model was then validated against textures extracted from high-frequency SAS imagery.

In this paper, a new detection method for high-resolution sonar imagery is developed using optimal Neyman-Pearson detection [15] and finite mixture models (FMM) for target plus \mathcal{K} -distributed background clutter. A new formulation for the estimation of the parameters of a FMM of \mathcal{K} -distributions based on stochastic expect-

*This work was supported by the NSWC PCD In-house Laboratory Independent Research program funded by the Office of Naval Research. Approved for public release; distribution is unlimited.

tation maximization (SEM) [14] is developed. A generalized log-likelihood ratio test (GLRT) is then developed for the FMM model and the detection results are then compared to scenarios where the standard \mathcal{K} , Gaussian, and Rayleigh distribution is assumed to model the background and target plus background. Our *detection hypothesis* in this non-Gaussian detection framework is that presence of objects in the sonar data leads to a change in the parameters of a FMM comparing to that of the background clutter only. The data set used in this study was provided by the Naval Surface Warfare Center Panama City Division (NSWC PCD) in Panama City, FL. The data set consists of real SAS image backgrounds with synthetically generated targets varying in target shape, type, aspect angle, range, inserted into the background.

This paper is organized as follows: Section 2 reviews the development of the \mathcal{K} -distribution. Section 3 develops the FMM for a mixture of \mathcal{K} -distributions with the associated parameter estimation method. Section 4 develops the generalized log-likelihood ratio test for the FMM \mathcal{K} -distributed detector. Section 5, presents the results using the detectors developed in Section 4 on SAS imagery with synthetic targets. Finally, conclusions and observations are offered in Section 6.

2. \mathcal{K} -DISTRIBUTION FOR MODELING BACKGROUND CLUTTER

The \mathcal{K} -distribution has been developed and motivated from the work in modeling the distribution of sea surface radar echoes. Ward [16] proposed a compound representation for modeling high resolution synthetic aperture radar (SAR) clutter based on a product of the Rayleigh and Gamma densities. The intuition behind this formulation was that high-resolution echoes created by SAR appear to be the modulation of uncorrelated noise by another background noise process with longer correlation lengths. This model was shown to fit the single-point statistics of SAR sea surface clutter. For our purposes here, this statistical model can also be applied to the envelope of sonar returns [12]. A step-by-step derivation of the \mathcal{K} -distribution beginning with the above assumptions of the compound distribution is provided here based on the notation in [17].

We assign $p_{X|Y}(x|y)$ to be the Rayleigh PDF with random parameter Y

$$p_{X|Y}(x|y) = \frac{x}{y^2} e^{-\frac{x^2}{2y^2}} u(x) \quad (1)$$

where $u(x)$ is the unit step function. Also, we assume $p_Z(z)$ to be the Gamma PDF with parameters ν and b

$$p_Z(z) = \frac{b^\nu}{\Gamma(\nu)} z^{\nu-1} e^{-bz} u(z). \quad (2)$$

where $\Gamma(\cdot)$ is the standard Gamma function. The square-root Gamma PDF $p_Y(y)$ is formed by the function relationship, $Y = \sqrt{Z}$ so that $p_Y(y) = 2yp_Z(y^2)$.

Thus, the functional form of the square-root Gamma PDF in terms of y is

$$p_Y(y) = \frac{2yb^\nu}{\Gamma(\nu)} y^{2\nu-2} e^{-by^2} u(y) \quad (3)$$

Let $p_X(x)$ be the PDF of the signal envelope. The compound representation follows from the use of marginalization over variable y :

$$p_X(x) = \int_{-\infty}^{\infty} p_{X|Y}(x|y) p_Y(y) dy. \quad (4)$$

Using (1) and (3) in (4), yields

$$p_X(x) = \frac{xb^\nu}{\Gamma(\nu)} \int_0^\infty y^{-2} y^{2\nu-2} e^{-\frac{x^2}{2y^2} - by^2} 2y dy. \quad (5)$$

Now, using integration by parts and simplifying the result we get,

$$p_X(x) = \frac{2\alpha}{\Gamma(\nu)} \left(\frac{\alpha x}{2} \right)^\nu K_{\nu-1}(\alpha x) u(x). \quad (6)$$

where $K_{\nu-1}(\cdot)$ is the modified Bessel function of the second kind [18]. This is the familiar PDF of the \mathcal{K} -distribution presented in [12, 16, 19] with shape parameter ν and scale parameter α .

3. FINITE MIXTURE MODEL

In our previous work [6], we used the assumption that when a target is present in a region of interest (ROI) within the sonar image it changes the shape and scale of the \mathcal{K} -distribution. Although this assumption resulted in good overall detection results, it does not accurately capture what is actually occurring statistically when a target is present in a \mathcal{K} -distributed background. If we simply model a target in a sonar image as a region containing all white pixels, representing the highlight, and all black pixels, representing the shadow, the distribution of the target will be a bimodal distribution consisting of two delta functions; one for the highlight pixels and one for the shadow pixels. Now, if the target is inserted into a \mathcal{K} -distributed background, the distribution of the target plus background is found by convolving the \mathcal{K} -distribution and that of the target distribution hence producing a mixture of two \mathcal{K} -distributions¹.

A finite mixture model (FMM) [20] is a probability distribution which is a convex combination of probability distributions. Assume that the random variable R is a mixture distribution, i.e.,

$$p_R(r|\Theta) = \sum_{i=1}^M \beta_i p_i(r|\theta_i) \quad (7)$$

where, $\beta = \{\beta_1, \dots, \beta_M\}$ is the set of mixing coefficients with $0 \leq \beta_i \leq 1$ and $\sum_{i=1}^M \beta_i = 1$. Moreover, θ_i is the vector of unknown parameters for the i^{th} distribution $p_i(r|\theta_i)$. If we define $\Theta = [\theta_1, \dots, \theta_M, \beta_1, \dots, \beta_M]^T$ as the vector containing all the parameters of the FMM one just needs to estimate Θ to estimate the PDF of R . The computation of maximum likelihood (ML) estimates of these parameters involves the maximization of the likelihood function, which may not be feasible analytically and suffers from numerical difficulties [14]. In order to get around this problem, the use of EM algorithm has been proposed [14, 20].

If we assume that we have N samples that are independent and identically distributed (i.i.d.), which is valid since we are using single point statistics, we can then write the following expression for the log-likelihood function for the FMM,

$$L(\theta) = \sum_{k=1}^N \ln p_R(r_k|\Theta) = \sum_{k=1}^N \ln \left[\sum_{i=1}^M \beta_i p_i(r_k|\theta_i) \right]. \quad (8)$$

The EM algorithm [14, 20, 21] provides a method to estimate the parameters of a FMM as an incomplete data problem and introduces a sequence $\{\Theta^t\}_{t=0}^\infty$ of parameter estimates by iteratively maximizing a pseudo-Likelihood function, i.e.,

$$\Theta^{t+1} = \arg \max_{\Theta \in \mathcal{O}} Q(\Theta|\Theta^t) \quad (9)$$

¹This model can be generalized to a more complex model for a target, e.g., a target with a dead-zone as well as a highlight and shadow

where O is the set of all possible parameter estimates and where

$$Q(\Theta|\Theta^t) = \sum_{k=1}^N \sum_{i=1}^M \tau_{ik}^t [\ln \beta_i^t + \ln p_i(r_k|\theta_i^t)], \quad (10)$$

$$\tau_{ik}^t = \frac{\beta_i^t p_i(r_k|\theta_i^t)}{p_R(r_k|\Theta^t)}, \quad \Theta \in O. \quad (11)$$

and the superscript t denotes the iteration index. In the context of FMM, the EM algorithm has been proven to converge to a stationary point of the log-likelihood function $L(\cdot)$ [14]. However, it may not converge to a global maximum and may exhibit long convergence time.

3.1. Stochastic Expectation Maximization

The Stochastic EM (SEM) [14] has been proposed to avoid the computation of the pseudo-Likelihood function $Q(\cdot|\cdot)$ and any related analytical maximization issues. This is done by integrating a stochastic sampling procedure in the estimation process which makes the sequence of parameter estimates a discrete time random process. This random process has been proven to be an ergodic and homogeneous Markov chain, converging to a unique stationary distribution which is expected to be concentrated around the global maxima of the log-likelihood function [14].

If we denote $\Sigma = \{\sigma_1, \dots, \sigma_M\}$ as the set of M different mixture components and assume the population label $s_k \in \Sigma$ of the k^{th} sample is unknown, we can then have the following definition of the complete and incomplete data vectors, respectively

$$\begin{aligned} \mathbf{w} &= (r_1, s_1, r_2, s_2, \dots, r_N, s_N), \\ \mathbf{v} &= (r_1, r_2, \dots, r_N). \end{aligned} \quad (12)$$

Assuming the pairs $\{(r_k, s_k) : k = 1, 2, \dots, N\}$ of random variables to be i.i.d. we can denote the parametric PDF of r_k conditioned on s_k ($p_{R|S}$), the parametric probability mass function (PMF) of s_k , (P_S), the parametric PMF of s_k conditioned on r_k ($P_{S|R}$), and the parametric joint density of (r_k, s_k) (p_{RS}), we can then define

$$P_S(s_k|\Theta) = \beta_i, \quad (13)$$

$$p_{R|S}(r_k|s_k, \Theta) = p_i(r_k|\theta_i), \text{ and} \quad (14)$$

$$p_{RS}(r_k, s_k|\Theta) = p_{R|S}(r_k|s_k, \Theta)P_S(s_k|\Theta), \quad (15)$$

where $\Theta \in O$, ($k = \{1, 2, \dots, N\}$, $i = \{1, 2, \dots, M\}$). The i.i.d. assumption yields the following expressions for the density functions of the incomplete and of the complete data vectors:

$$p_V(\mathbf{v}|\Theta) = \prod_{k=1}^N p_R(r_k|\Theta), \quad (16)$$

$$p_W(\mathbf{w}|\Theta) = \prod_{k=1}^N p_{R|S}(r_k|s_k, \Theta)P_S(s_k|\Theta), \quad (17)$$

$$p_{W|V}(\mathbf{w}|\mathbf{v}, \Theta) = \prod_{k=1}^N P_{S|R}(s_k|r_k, \Theta). \quad (18)$$

Given an observed incomplete data realization, SEM computes a random sequence $\{\Theta^t\}_{t=0}^{\infty}$, by performing at the t^{th} iteration the following processing steps:

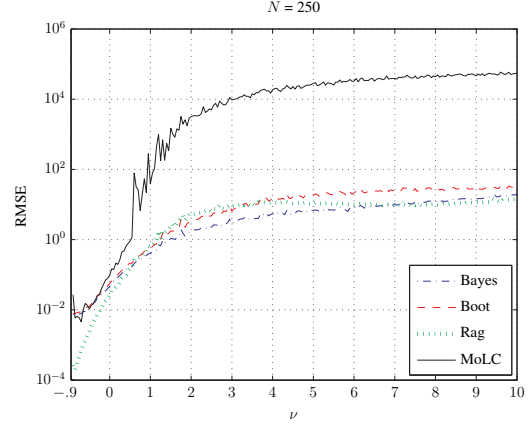


Fig. 1. RMSE of ν Estimators for 250 Samples.

- **E-step:** compute the conditional complete data density $p_{w|v}(\cdot|v, \Theta^t)$ corresponding to the current parameter estimate $\Theta^t \in O$, ($k = \{1, 2, \dots, N\}$, $i = \{1, 2, \dots, M\}$), i.e.,

$$\begin{aligned} P_{S|R}(s_k|r_k, \Theta^t) &= p_{R|S}(r_k|s_k, \Theta^t) \frac{P_S(s_k|\Theta^t)}{p_R(r_k|\Theta^t)} \\ &= \frac{\beta_i^t p_i(r_k|\theta_i^t)}{p_R(r_k|\Theta^t)} = \tau_{ik}^t. \end{aligned} \quad (19)$$

- **S-step:** sample a complete data realization \mathbf{w}^t according to the conditional density computed in the **E-step**. This is done by sampling a label s_k^t for each k^{th} sample according to the current estimated posterior probability distribution $\{\tau_{ik}^t : i = 1, 2, \dots, M\}$ of the pixel ($k = \{1, 2, \dots, N\}$), thus implicitly partitioning the data into M subsets.
- **M-step:** update the parameter estimate, by computing, according to each partition generated by the S-step, a standard supervised ML estimate $\Theta^{t+1} \in O$

$$\beta_i^{t+1} = \frac{|Q_{it}|}{N} \quad (20)$$

$$\theta_i^{t+1} = \arg \max_{\theta_i \in O_i} \sum_{k \in Q_{it}} \ln p_i(r_k|\theta_i), \quad (21)$$

for $i = \{1, 2, \dots, M\}$ and where $Q_{it} = \{k : s_k^t = \sigma_i\}$ is the index set of the samples assigned to the component σ_i , $\forall i = \{1, 2, \dots, M\}$.

3.2. Parameter Estimation for FMM of \mathcal{K} -distributions

Since we know that there is no closed form to the ML solution for the parameter estimation of a \mathcal{K} -distribution [22], the **M-step** in the SEM procedure causes difficulty when estimating the parameters of a FMM when the component densities are assumed to be \mathcal{K} -distributed as would be in our target plus signal model. Therefore, an experimental study was conducted to compare the performance and feasibility of different parameter estimators for the \mathcal{K} -distribution for substitution for the ML estimator in the **M-step**. Several methods were compared including Raghavan's Method of Moments (MoM) [23], method of log-cumulants (MoLC) [24],

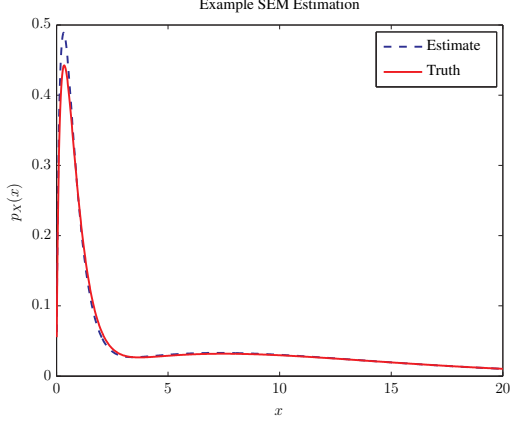


Fig. 2. Example FMM \mathcal{K} -distribution with SEM Estimate.

Bayesian MoM, and Bootstrapped MoM [22]. Figure 1 presents the root mean squared error (RMSE) of the four estimators for $\nu = [-0.9 : 10]$ for a sample size of 250. These results were formed over 1000 Monte-Carlo iterations and from these results we decided to utilize the Bayesian Method of Moments (MoM) parameter estimation method in place of the ML estimator in the **M-step** of the iterative SEM estimation process. We chose this method due to its nice estimation properties over the range of ν and for small sample sizes. Therefore, our proposed method is the same as above except we change the **M-step** to use Bayesian MoM to calculate θ_i^{t+1} in (21) for the \mathcal{K} -distribution of each partition.

An example of using the above algorithm for estimating the parameters of a FMM of \mathcal{K} -distributions is presented in Figure 2. The truth is shown by the solid curve and is a two component mixture with $\beta = [1/2, 1/2]$ and $\Theta = [\nu_1, \alpha_1, \nu_2, \alpha_2] = [0.1, 0.5, 2, 4]$ and the estimate is shown by the dashed curve. As can be seen, the algorithm does quite well in estimating the distribution with the estimate parameters being $\hat{\beta} = [0.4955, 0.5045]$, $\hat{\Theta} = [0.26, 0.41, 2.096, 3.85]$. The estimation algorithm was also ran for 1000 Monte Carlo trials with a mean-squared error of 0.076 and standard error of 0.52.

4. GENERALIZED LIKELIHOOD RATIO TEST

In this section we derive the GLRT for the detection of targets in sonar imagery with \mathcal{K} -distributed background. Our detection problem is the decision between two hypotheses which is either a \mathcal{K} -distributed background alone (H_0) or signal plus background (H_1) i.e., a FMM of \mathcal{K} -distributions. Thus, our hypotheses can be defined as

$$\begin{aligned} H_0 : z &\sim p_0(z|\theta_0) \\ H_1 : z &\sim p_1(z|\Theta_1). \end{aligned} \quad (22)$$

where z is our observation and $p_0(z|\theta_0) \sim \mathcal{K}(\alpha_0, \nu_0)$ and $p_1(z|\Theta_1) = \sum_{i=1}^M \beta_i p_i(z|\theta_i)$, where $p_i(y|\theta_i)$ is \mathcal{K} -distributed.

Therefore, the GLRT for this model is

$$\Lambda(z) = \max_{\theta_0, \Theta_1} \ln \frac{\sum_{i=1}^M \beta_i p_i(z|\theta_i)}{p_0(z|\theta_0)} \underset{H_0}{\overset{H_1}{\geq}} \lambda \quad (23)$$

where we maximize over the entire parameter space and compare against a predetermined decision threshold, λ . If the GLRT is greater

than λ we declare the sample as a target sample and if it is less than λ we declare the sample as background.

The modified Bessel function of the second kind in the \mathcal{K} -distribution can be well-approximated [25] by, $K_\alpha(b) \approx \frac{e^{-b}}{\sqrt{\frac{2}{\pi}b}}$, $b \gg \alpha$.

a. Therefore, we can simply write the GLRT as

$$\begin{aligned} \Lambda(z) &\approx \max_{\theta_0, \Theta_1} \ln \left(\sum_{i=1}^M \beta_i \frac{2\alpha_i}{\Gamma(\nu_i)} \left(\frac{\alpha_i z}{2}\right)^{\nu_i} \frac{e^{-\alpha_i z}}{\sqrt{\frac{2}{\pi}(\alpha_i z)}} \right) \\ &\quad - \ln(2\alpha_0) + \ln(\Gamma(\nu_0)) - \nu_0 \ln(\alpha_0 z) + \nu_0 \ln 2 \\ &\quad + \alpha_0 z + \frac{1}{2} \ln \left(\frac{2}{\pi} \alpha_0 z \right). \end{aligned} \quad (24)$$

Hence, avoiding the numerical difficulties of the computation of $M + 1$ Bessel functions for each sample and greatly simplifying the functional form of the GLRT.

5. SIMULATION RESULTS

An experiment was conducted to show the performance of the developed detector (24) versus the \mathcal{K} -distributed detector in [6] which models the difference in hypotheses as a change in the parameters of the \mathcal{K} -distribution and also versus the standard Rayleigh and Gaussian cases for sonar imagery data. Specifically, we want to show that the GLRT in (24) for FMM \mathcal{K} -distributions under H_1 has higher performance over the detectors developed in [6]. Moreover, we would like to study the sensitivity of the GLRT to different signal-to-clutter ratio (SCR) levels, where SCR is defined to be the target highlight intensity level relative to the mean background level of the image,

The sonar image database used in the test was developed by NSWC PCD to test detector performance for various target shapes in realistic seabed environments. Various targets were placed in a real sonar image at different orientations and an acoustic scattering model was used to generate raw sonar returns which is the beam-formed into high-resolution images [26]. This generation method incorporates both the physical attributes of the target and the context of the seabed by using the amplitude pixel values in the sonar image as a reflectivity map for scattered sound energy. Targets were generated from four classes, namely a box, cone, sphere, and cylinder and are inserted into backgrounds from a high-resolution high-frequency imaging sonar with varying bottom difficulty. There were 11 different background types with the four targets in 13 different arrangements, giving a total of 143 images. From the images 572 background snippets and 572 target snippets were created. Therefore, from the data set under H_0 the image is pure background and under H_1 we have target plus background. For each snippet the SCR was varied from 3 dB to 20 dB, hence allowing us to see the targets in different target strength scenarios.

The detectors were trained on a set of 286 target and 286 background snippets with varying SCR and the optimum threshold was determined from this training set by forming the receiver operating characteristic (ROC) curve for the training set and choosing the threshold that corresponds to the knee point (where $P_D + P_{FA} = 1$). The optimum threshold was set at $\lambda = 1.5$. It was assumed that under H_1 the FMM contained $M = 2$ components and was trained using the developed SEM algorithm in Section 3.2. The motivation behind using $M = 2$ is to use a simple target model consisting of only highlight and shadow structures which has a bimodal distribution of two delta functions. In the detection process, the GLRT is calculated using (24) for each pixel in an image snippet. The log-likelihood value is then compared against the detection threshold (λ) and either

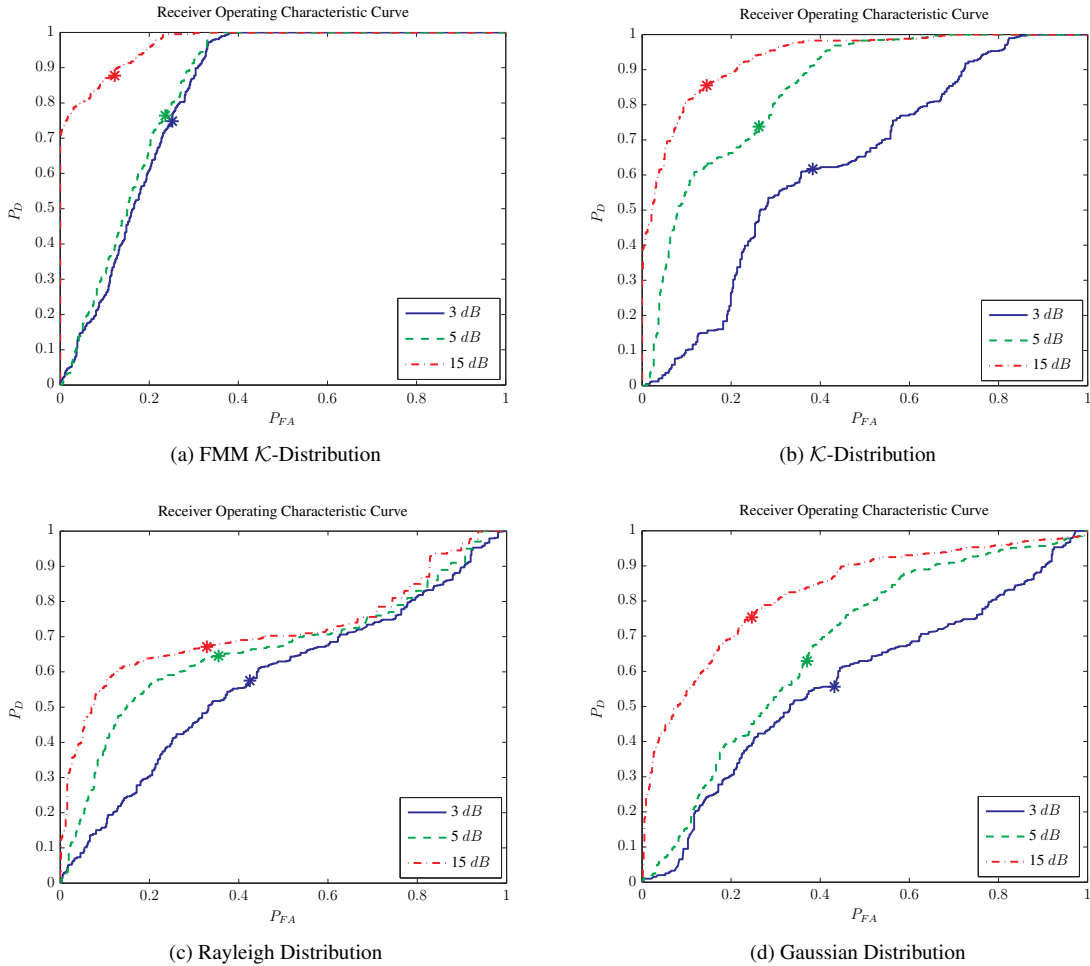


Fig. 3. Receiver Operating Characteristic Curves for Different Statistical Distribution Assumptions for Different SCR.

a background pixel or target pixel is declared. Using the calculated log-likelihood values, ROC curves were generated by varying λ .

5.1. Performance Under Different SCR Calculations

From the log-likelihood values a study on the effect of SCR on the detection performance was conducted. Using the calculated log-likelihood values a set of ROC curves were generated for each SCR in the dataset. Figure 3a presents the ROC curves for the FMM detector for 3, 5, and 15 dB SCR with the knee points being marked by ‘*’. The corresponding P_D values are presented in Table 1.

	FMM \mathcal{K} -dist	\mathcal{K} -dist	Rayleigh	Gaussian
3 dB	0.74	0.61	0.57	0.54
5 dB	0.76	0.73	0.64	0.62
15 dB	0.87	0.85	0.67	0.75

Table 1. Knee Point Probability of Detection for ROC Curves in Figure 3

For a complete comparison of the performance of the FMM \mathcal{K} -distributed detector, ROC curves were also generated for both the standard \mathcal{K} -distribution as well as the Rayleigh and the Gaussian

cases. The ROC curves were generated the same way as the FMM case except the log-likelihood ratio was calculated using the corresponding equations in [6]. Figures 3b-3d present the ROC curves for these cases, respectively with the knee points being marked by ‘*’. The corresponding P_D values are presented in Table 1. As expected for all detectors we notice an increase in the performance as SCR increases. For 15 dB SCR the FMM has a much higher P_D for a lower P_{FA} , than those of the other three detectors. Moreover, the FMM detector has the best performance for the low SCR cases due to the ability of our FMM of \mathcal{K} -distributions to correctly model the target plus background case under H_1 . It is also interesting to note here that the Gaussian detector requires a high SCR to produce any performance similar to the \mathcal{K} -distributed based detectors.

6. CONCLUSION

In this paper, we developed a FMM \mathcal{K} -distributed detector for the detection of objects in sonar images that contain \mathcal{K} -distributed backgrounds. It has been shown that by using an approximation to the Bessel function we can formulate an explicit, concise GLRT for a model using a FMM consisting of \mathcal{K} -distributed random variables. Our experiments on the SAS image data set provided by the NSWC

PCD demonstrated good detection performance across all SCR's over those of the standard K -distributed as well as the Rayleigh, and Gaussian-based detector. Overall, the FMM K -distributed detector shows promise in improving the detection rate while lowering the false alarm rate in the detection of underwater objects from sonar imagery.

7. REFERENCES

- [1] S. Reed, Y. Petillot, and J. Bell, "An automatic approach to the detection and extraction of mine features in sidescan sonar," *IEEE Journal of Oceanic Engineering*, vol. 28, no. 1, pp. 90–105, Jan 2003.
- [2] G. J. Dobeck, "Fusing sonar images for mine detection and classification," *Proc. SPIE*, vol. 3710, pp. 602–614, April 1999.
- [3] —, "Image normalization using the serpentine forward-backward filter: application to high-resolution sonar imagery and its impact on mine detection and classification," *Proc. SPIE*, vol. 5734, pp. 90–110, April 2005.
- [4] T. Aridgides and M. F. Fernandez, "Automatic target recognition algorithm for high resolution multi-band sonar imagery," *Proc. of MTS/IEEE Oceans 2008 Conference*, pp. 1–7, Sep. 2008.
- [5] J. D. Tucker, N. Klausner, and M. R. Azimi-Sadjadi, "Target detection in m-disparate sonar platforms using multichannel hypothesis testing," *Proc. of MTS/IEEE Oceans 2008 Conference*, pp. 1–7, Sep. 2008.
- [6] J. D. Tucker and M. R. Azimi-Sadjadi, "Neyman Pearson detection of K -distributed random variables," *Proc SPIE*, vol. 7664, pp. Q1–Q12, April 2010.
- [7] C. Ciany and W. Zurawski, "Enhanced ATR using Fisher fusion techniques with application to side-looking sonar," *Proc SPIE*, vol. 7664, pp. 1Z–10Z, 2010.
- [8] T. Aridgides and M. Fernandez, "Image-based ATR utilizing adaptive clutter filter detection, LLRT classification, and volterra fusion with application to side-looking sonar," *Proc. SPIE*, vol. 7664, pp. 1R–11R, March 2010.
- [9] T. Aridgides, P. Libera, M. Fernandez, and G. J. Dobeck, "Adaptive filter/feature orthogonalization processing string for optimal LLRT mine classification in side-scan sonar imagery," *Proc. SPIE*, vol. 2765, pp. 110–121, April 1996.
- [10] J. D. R. Vera, E. Corias, J. Groen, and B. Evans, "Automatic target recognition in synthetic aperture sonar images based on geometrical feature extraction," *EURASIP Journal on Advances in Signal Processing*, vol. 2009, no. 109438, pp. 1–9, 2009.
- [11] S. Stanic, R. Goodman, K. Briggs, N. P. Chotiros, and E. Kennedy, "Shallow-water bottom reverberation measurements," *IEEE Journal of Oceanic Engr.*, vol. 23, pp. 203–210, 1998.
- [12] D. Abraham and A. Lyons, "Novel physical interpretations of K -Distributed reverberation," *IEEE Journal of Oceanic Engineering*, vol. 27, no. 4, pp. 800–813, October 2002.
- [13] J. T. Cobb, K. C. Slatton, and G. J. Dobeck, "A parametric model for characterizing seabed textures in synthetic aperture sonar images," *IEEE Journal of Oceanic Engineering*, vol. 35, no. 2, pp. 250–266, April 2010.
- [14] G. J. McLachlan and T. Krishnan, *The EM Algorithm and Extensions*. Wiley, 2008.
- [15] H. L. Van Trees, *Detection, Estimation, and Modulation Theory Part I*. John Wiley and Sons, 1968.
- [16] K. Ward, C. Baker, and S. Watts, "Maritime surveillance radar part 1: radar scattering from the ocean surface," *IEE Proc. Radar, Sonar Navig.*, vol. 137, no. 2, April 1990.
- [17] J. T. Cobb and K. C. Slatton, "A parameterized statistical sonar image texture model," *Proc. SPIE*, vol. 6953, pp. K1–K12, 2008.
- [18] I. Gradshteyn and I. Ryzhik, *Table of Integrals, Series, and Products*. Academic Press, 1965.
- [19] E. Jakeman and P. Pusey, "A model for non-Rayleigh sea echo," *IEEE Trans. on Antennas and Propagation*, vol. AP-24, no. 6, pp. 806–814, November 1976.
- [20] G. J. McLachlan and D. Peel, *Finite Mixture Models*. Wiley, 2000.
- [21] G. J. McLachlan and K. E. Basford, *Mixture Models: Inference and Applications to Clustering*. Marcel Dekker, 1988.
- [22] D. A. Abraham and A. P. Lyons, "Reliable methods for estimating the K -distribution shape parameter," *IEEE Journal of Oceanic Engineering*, vol. 35, no. 2, pp. 288–302, April 2010.
- [23] R. S. Raghavan, "A method for estimating parameters of K -distributed clutter," *IEEE Trans. Aerosp. Electron. Syst.*, vol. 26, no. 3, pp. 348–357, Mar 1991.
- [24] J. M. Nicolas and F. Tupin, "Gamma mixture modeled with "second kind statistics" application to SAR image processing," *Proc. of IEEE IGARSS '02*, vol. 4, pp. 2489–2491, June 2002.
- [25] P. Kasperkovitz, "Asymptotic approximations for modified Bessel functions," *Journal of Math Physics*, vol. 21, no. 1, pp. 6–13, January 1980.
- [26] G. Sammelmann, J. Christoff, and J. Lathrop, "Synthetic images of proud targets," *Proc. of MTS/IEEE Oceans 2006 Conference*, pp. 1–6, Sep. 2006.